Design of silicate nanostructures by interlayer alkoxysilylation of layered silicates (magadiite and kenyaite) and subsequent hydrolysis of alkoxy groups†

Dai Mochizuki[a] and Kazuyuki Kuroda*[abc]

Received (in Montpellier, France) 5th October 2005, Accepted 13th December 2005
First published as an Advance Article on the web 3rd January 2006
DOI: 10.1039/b514157e

Silica nanostructures are sophisticatedly designed by interlayer alkoxysilylation of layered silicates (magadiite and kenyaite) with alkoxytrichlorosilanes and the subsequent hydrolysis of alkoxy groups. The dichlorosilyl groups of alkoxytrichlorosilanes [(RO)ClSiCl$_2$] were reacted onto two neighboring Si–OH groups on the surface of the layered silicates to form a bridge, leaving two functional (Si–OR and Si–Cl) groups on the bridge. The remaining bifunctional groups were almost completely hydrolyzed to transform into Si–OH groups. Depending on the solvent for hydrolysis, the hydrolyzed product derived from magadiite forms either a new 3-D silicate structure by condensation of interlayer silanol groups or a new 2-D silicate structure by geminal Si–OH groups remaining immobilized on both sides of the silicate layers. The 3-D silicate structure exhibits microporosity (130 m^2 g^{-1}) and hydrophilic behavior. On the other hand, the hydrolyzed product from kenyaite takes only a 2-D silicate structure, even when the solvents for hydrolysis were completely evaporated.

Introduction

Ordered nanostructured silicates, such as zeolites and layered silicates, have received broad interest in both basic chemistry and various applications including catalysis and adsorption.[1,2] Their crystalline silica frameworks have mainly been synthesized hydrothermally.[3–6] To design novel silica frameworks and nanospaces created by utilizing those networks, it is desirable to establish a versatile and soft-chemical methodology.

Much effort has been dedicated to increase the variety and availability of silica nanostructures. Aluminium-free layered silicates with two dimensional (2-D) structures are potential scaffolds for construction of nanostructured silicas because of their high crystallinity with expandable interlayer spaces. To create a three dimensional (3-D) silicate structure, transformation of layered silicates into zeolites has been achieved by a hydrothermal treatment.[7–10] Unfortunately, this method provides silica structures which have a disadvantaged structural relationship between the layer motifs and the products. A topotactic conversion from layered silicates to 3-D zeolitic structures having the complete structural relationship has recently been realized by careful calcination.[11–18] However, this method basically imposes a limitation on the use of other layered silicates because of the difficulty in the connection of Si–OH groups between adjacent layers. Kosuge *et al*. and other researchers reported the pillaring of the interlayer spaces by condensation of silicic acids or other metal oxides in the presence of surfactants to form porous structures.[19–22] However, the interlayer structures created by pillaring are amorphous due to the random condensation of various silica species.

We have exploited a novel approach toward construction of nanostructured silicas using silylation of layered silicates as a sort of "building-up" approach. Silylation of layered silicates can immobilize silyl groups on the interlayer surface as a monolayer.[23–39] Rojo and Ruiz-Hitzky[23] and we[36] have reported that silylation of kanemite (single-layered silicate) and magadiite (multi-layered silicate) with dichloro- or trichloroorganosilanes generated new siloxane networks by covalent bonding to the interlayer Si–OH groups. However, these silylated products are not suitable for the construction of novel silica nanostructures composed of SiO_4 tetrahedra because Si–C bonds of silyl groups cannot be cleaved under mild conditions. To construct such crystalline silica nanostructures, we have focused on the silylation of layered silicate using *alkoxy*chlorosilanes [(RO)$_n$SiCl$_{4-n}$; R = alkyl, n = 1 or 2] as a silylating agent. The Si–Cl groups of alkoxychlorosilanes react with Si–OH groups on the interlayer surface due to their higher reactivity, rather than with Si–OR groups, resulting in the immobilization of Si–OR groups on the interlayer surface. Then, Si–OR groups can be transformed into Si–OH groups by hydrolysis. We reported the formation of a crystalline silicate structure through the alkoxysilylation of layered octosilicate having a suitable silicate structure (stable structure, alignment of Si–OH groups) for regular grafting of silyl groups.[34] More recently, we succeeded in manipulation of 2-D/3-D silica nanostructures by hydrolysis of alkoxy groups

[a] *Department of Applied Chemistry, Waseda University, Ohkubo-3, Shinjuku-ku, Tokyo 169-8555, Japan. E-mail: kuroda@waseda.jp; Fax: +81-3-5286-3199; Tel: +81-3-5286-3199*
[b] *CREST, Japan Science and Technology Agency, Honcho 4-1-8, Kawaguchi-shi, Saitama 332-0012, Japan*
[c] *Kagami Memorial Laboratory for Materials Science and Technology, Waseda University, Nishiwaseda 2-8-26, Shinjuku-ku, Tokyo 169-0051, Japan*

† Electronic supplementary information (ESI) available: SEM images. See DOI: 10.1039/b514157e

on alkoxysilylated layered octosilicate and subsequent condensation.[39] The new 2-D silicate nanostructure was fabricated by hydrolysis with a mixture of dimethylsulfoxide (DMSO)–water, and the mixture suppresses the interlayer condensation due to the low volatility of interlayer DMSO. On the other hand, a 3-D silicate nanostructure, which was induced by the condensation of adjacent layers, was fabricated by hydrolysis with a mixture of acetone–water, although the formed 3-D micropores derived from layered octosilicate are not stable if occluded acetone molecules are completely removed. However, in contrast to the above approaches, our new methodology can be extended to other layered silicates for designing new crystalline nanostructures.

Herein, we report the synthesis of novel silica nanostructures by silylation of magadiite and kenyaite. For the precise control of the silica frameworks, the high flexibility of single silicate layers of kanemite is disadvantageous. The silicate structures of magadiite and kenyaite, having thicker silicate layers,[40–42] are stable for silylation. Although the crystal structures have not yet been determined,[43–45] the crystalline nature has been characterized by various methods such as FTIR, ^{29}Si NMR, and ^{1}H NMR.[46,47] In particular, the distance of neighboring Si–OH groups for magadiite was determined to be 0.25 nm[46] which is appropriate for the controlled grafting of silyl groups by the reaction with two Si–Cl groups of one alkoxychlorosilane molecule. Moreover, the interlayer surface of magadiite has been expected to be uneven.[47] The uneven structure will contribute to the formation of 3-D micropore after the condensation of Si–OH groups. Kenyaite has a thicker layer than magadiite, and the comparison between magadiite and kenyaite may contribute to the further understanding of the interlayer surfaces of these layered silicates as well as their reactivities. Consequently, these layered silicates should be appropriate for interlayer modification and subsequent transformation to crystalline 3D frameworks. This paper shows a significant step toward the precise design of new silica nanostructures with possible extension to various layered silicates.

Experimental

Syntheses

Na-magadiite, Na-kenyaite, and C_{16}TMA-exchanged intermediates. Na-magadiite (Na-Mag; $Na_2Si_{14}O_{29}\cdot nH_2O$) and Na-kenyaite (Na-Ken, $Na_2Si_{20}O_{41}\cdot nH_2O$) were synthesized by the methods reported previously.[48,49] For the magadiite synthesis SiO_2 (special grade, Wako Chemicals), NaOH, and distilled water were mixed in a ratio of $SiO_2 : NaOH : H_2O$ = 1 : 0.23 : 18.5. The mixture was then heated at 150 °C for 2 days in a sealed Teflon vessel. The resulting suspension was filtered, the residue was washed with a dilute NaOH aqueous solution (pH = ~9), and the product was dried at 40 °C. For the kenyaite synthesis SiO_2, NaOH, Na_2CO_3, and distilled water were mixed in a ratio of $SiO_2 : NaOH : Na_2CO_3 : H_2O$ = 30 : 1 : 2 : 600. The subsequent procedure was the same as that for magadiite. Hexadecyltrimethylammonium-exchanged intermediates of the silicates were prepared by the ion exchange reaction of interlayer sodium cations with hexadecyltrimethylammonium ions.[25] Na-Mag or Na-Ken (12 g) was dispersed in an aqueous solution of hexadecyltrimethylammonium chloride [$C_{16}H_{33}N(CH_3)_3Cl$, C_{16}TMACl] (0.1 mol L^{-1}, 400 ml). The mixture was stirred at room temperature for 24 h, and then centrifuged to remove the supernatants. This procedure was repeated three times for complete ion exchange. The resulting slurry was washed with water, and air-dried at room temperature. The products are denoted as C_{16}TMA-Mag and C_{16}TMA-Ken, respectively.

Synthesis of dodecoxytrichlorosilane. Dodecoxytrichlorosilane ($C_{12}H_{25}OSiCl_3$) was synthesized by a method similar to that reported previously.[25] *n*-Dodecyl alcohol ($C_{12}H_{25}OH$, Tokyo Kasei Co.) was added dropwise to a vigorously stirred mixture of $SiCl_4$ (Tokyo Kasei Co.) and hexane ($SiCl_4$/$C_{12}H_{25}OH$ = 1.3) under a N_2 flow. The mixture was allowed to react at room temperature for 1 h, yielding a mixture of $(C_{12}H_{25}O)_mSiCl_{4-m}$ (m = 0 ~ 4). Dodecoxytrichlorosilane (m = 1) was purified by distillation (0.1 Torr, bp; ~110 °C). The ^{29}Si NMR spectrum of the sample exhibited a single signal at −38.5 ppm assignable to $C_{12}H_{25}OSiCl_3$.[50] In addition, the ^{13}C NMR spectrum showed the signals assigned to dodecoxy groups, and the signal of α carbon (Si*O*C) appeared at 66.6 ppm, being shifted from that of $C_{12}H_{25}OH$ (62.5 ppm in $CDCl_3$).

Silylation. C_{16}TMA-Mag or C_{16}TMA-Ken (1.5 g) dispersed in dehydrated dichloromethane (30 mL) containing dehydrated pyridine (4 mL) was mixed with an excess amount (20 mmol) of dodecoxytrichlorosilane. The mixture was stirred at room temperature for 1 day under a N_2 atmosphere. The solid sample was filtered and washed with dichloromethane to remove unreacted silylating reagents, pyridine hydrochloride, and deintercalated C_{16}TMACl. The resulting products were dried *in vacuo* to yield the silylated samples denoted as **1(Mag)** or **1(Ken)**, respectively (Fig. 1).

Hydrolysis of alkoxy groups. The silylated sample **1(Mag)** or **1(Ken)** (0.5 g) was added to a mixture of DMSO (40 mL), H_2O (10 ml), and pyridine (1.0 ml). After stirring for 1 day, the mixture was centrifuged, and the solid components were washed with a mixture of DMSO and water. The products after drying *in vacuo* for 2 h are designated as **2(Mag)** and **2(Ken)** (Fig. 1). To form a 3-D silicate framework, the silylated sample **1(Mag)** or **1(Ken)** was also hydrolyzed with a mixture of acetone and water by a procedure similar to that described above. The samples were denoted as **3(Mag)** and **3(Ken)**, respectively.

Analyses

Powder X-ray diffraction (XRD) measurements were performed on a Rigaku Rint 2000 powder diffractometer with monochromated Cu Kα radiation (λ = 0.154 05 nm). Thermogravimetry (TG) was carried out with a Rigaku Thermo Plus2 instrument under a dry air flow at a heating rate of 10 °C min^{-1}, and the amounts of SiO_2 fractions in the products were determined by the residual weight after heating to 900 °C. The amounts of organic constituents were determined by CHN analysis (Perkin-Elmer PE-2400). Solid-state ^{29}Si MAS NMR spectra were recorded on a JEOL JNM-CMX-400

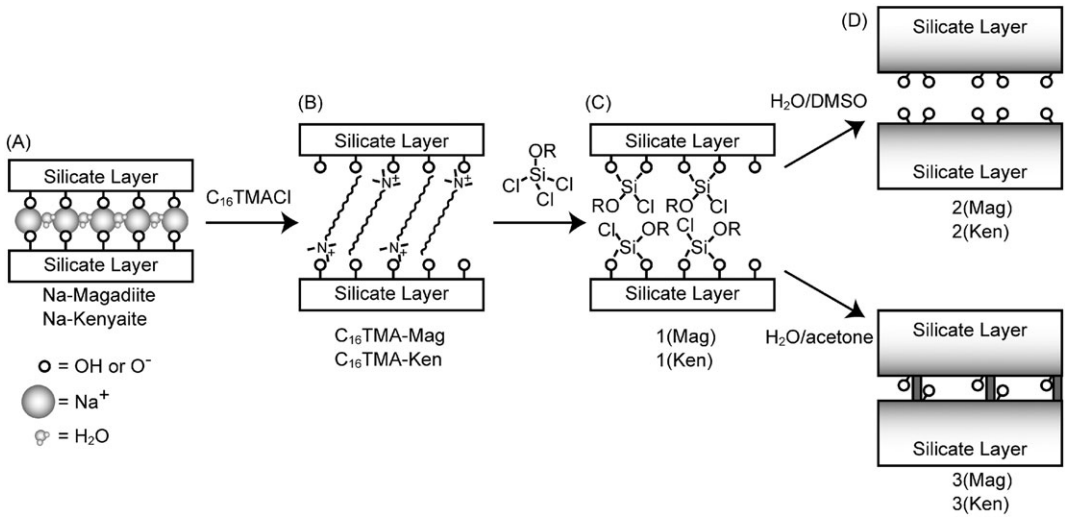

Fig. 1 Expected representation of (A) layered silicates, (B) intermediates, (C) silylated products, and (D) hydrolyzed products.

spectrometer at a resonance frequency of 79.42 MHz. We confirmed that the signals were fully relaxed under a recycle delay of 600 sec with a 30° pulse for samples from magadiite and 18° pulse for samples from kenyaite so that quantitative analysis was possible. The samples were put into 7.5 mm (or 5 mm) zirconia rotors and spun at 5 kHz. Solid-state ^{13}C CP/MAS NMR spectra were recorded on the same spectrometer at a resonance frequency of 100.40 MHz and a recycle delay of 5 s. The ^{29}Si and ^{13}C chemical shifts were referenced to tetramethylsilane at 0 ppm. Argon adsorption measurements were carried out on a Quantachrome Autosorb-1MP. Before the adsorption measurements, samples were outgassed at 200 °C for 3 h. The BET surface areas were calculated from the adsorption data in the relative pressure range around 0.1. Water vapor adsorption isotherms at 298 K were collected on a Belsorp 18 (Bel Japan, Inc.). Samples were outgassed at 120 °C for 3 h prior to the measurements. The scanning electron microscopic (SEM) images were obtained with a JEOL JSM-5500LV microscope at an accelerating voltage of 25 kV.

Results and discussion

Silylation of layered silicates

Dodecoxysilylated magadiite and kenyaite were obtained through the reaction of the hexadecyltrimethylammonium intermediates with dodecoxytrichlorosilane. The XRD patterns of Na-magadiite, C_{16}TMA-Mag, and **1(Mag)** are shown in Fig. 2a–c, respectively, and those of Na-kenyaite, C_{16}TMA-Ken and **1(Ken)** are shown in Fig. 3a–c. The basal spacings of the silylated derivatives [**1(Mag)**; d_{010} = 2.51 nm, **1(Ken)**; d_{010} = 3.06 nm] decrease from those of the C_{16}TMA-intermediates. The absence of nitrogen in the silylated samples was confirmed, whereas the nitrogen contents due to C_{16}TMA ions in the C_{16}TMA-intermediates were 1.8 and 1.5 wt%, respectively (Table 1). These indicate the reactions of layered silicates with dodecoxytrichlorosilane through the complete removal of C_{16}TMA ions. The several peaks at the high angle region of the silylated samples demonstrate the retention of the crystal structure after the silylation. The amounts of silyl groups were evaluated to be 0.5 per reactive site (Si–OH or Si–O^-) on the basis of the CHN and thermogravimetric data (Table 1), which is similar to the case of octosilicate. These values suggest the reaction of one silylating agent with two reactive sites as described below.

The information on the alkoxy groups was obtained by ^{13}C CP/MAS NMR spectra (Fig. 4a and 5a). The spectra of **1(Mag)** and **1(Ken)** show the signals assigned to dodecoxy

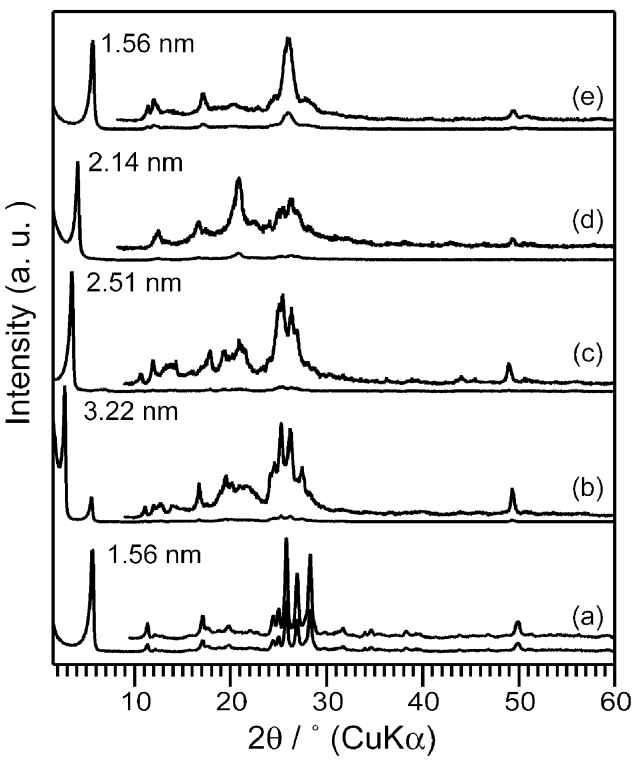

Fig. 2 XRD patterns of (a) Na-Mag, (b) C_{16}TMA-Mag, (c) **1(Mag)**, (d) **2(Mag)**, and (e) **3(Mag)**.

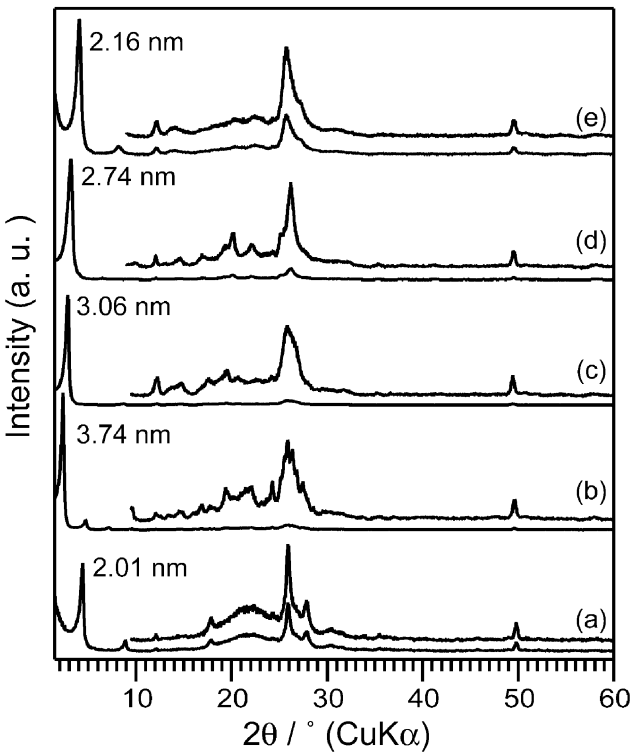

Fig. 3 XRD patterns of (a) Na-Ken, (b) C_{16}TMA-Ken, (c) **1(Ken)**, (d) **2(Ken)**, and (e) **3(Ken)**.

groups. The signals at 65 ppm are assigned to the α carbon of the dodecoxy group, revealing that the alkoxy groups are grafted onto the silica surfaces.[51] The signals at 33 ppm indicate the all-*trans* conformation of the interior methylene chains as found for alkoxysilylated octosilicate.[39] The interlayer galleries (1.36 nm and 1.30 nm), calculated from the subtraction of the layer thickness of the protonated layered silicates from the basal spacings of the samples, are also similar to that of the dodecoxysilylated octosilicate (1.31 nm), suggesting similar alignments of the interdigitated alkyl groups. The interlayer gallery of silylated products is known to be affected by the density of interlayer silyl groups.[36] Based on the similar interlayer galleries, we can assume that the densities of silyl groups in the interlayer surfaces for magadiite and kenyaite are approximately equivalent to that of octosilicate.

Table 1 Amounts of alkoxy groups in the products

	Mass %C	Mass %N	$\%SiO_2$	Amount of alkoxy groups/ (SiOH + SiO–)[a]
C_{16}TMA-Mag	30.8	1.8	57.3	
1(Mag)	20.0	0.0	71.3	0.47
2(Mag)	6.8	0.0	79.2	
3(Mag)	3.9	0.2	92.0	
C_{16}TMA-Ken	25.8	1.5	67.5	
1(Ken)	15.2	0.0	79.3	0.50
2(Ken)	8.6	0.0	67.8	
3(Ken)	6.4	0.0	94.4	

[a] Evaluated by ^{29}Si MAS NMR and thermogravimetry.

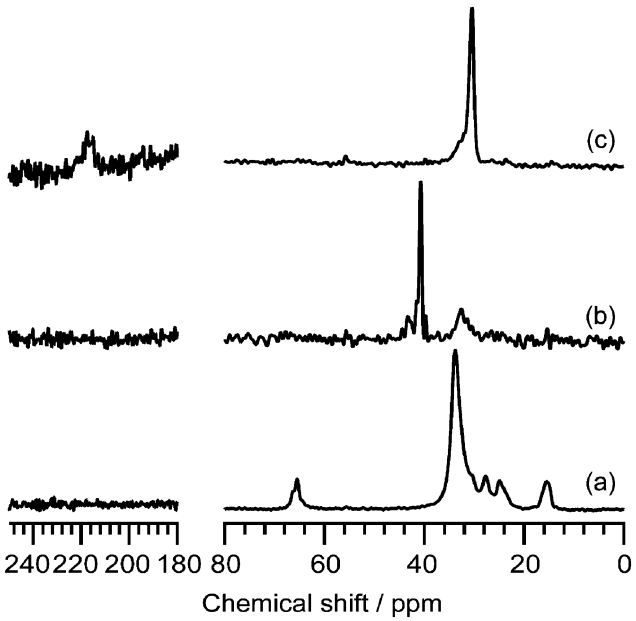

Fig. 4 ^{13}C CP/MAS NMR spectra of (a) **1(Mag)**, (b) **2(Mag)**, and (c) **3(Mag)**.

To confirm the controlled grafting of the Si species onto the interlayer surface, the ^{29}Si MAS NMR spectra of the silylated samples were measured. The spectra of C_{16}TMA-Mag (Fig. 6a) and C_{16}TMA-Ken (Fig. 7a) show several signals in the Q^3 [$Si(OSi)_3(O^-)$] region at −100 ppm and the Q^4 [$Si(OSi)_4$] region from −109 to −117 ppm. The intensity ratio of these signals (Q^4/Q^3) is 3 for the C_{16}TMA-Mag and 5.25 for C_{16}TMA-Ken, respectively (Table 2) and these values are almost same as those of Na-Mag and Na-Ken. The spectra of the silylated samples show new signals at around −84 ppm

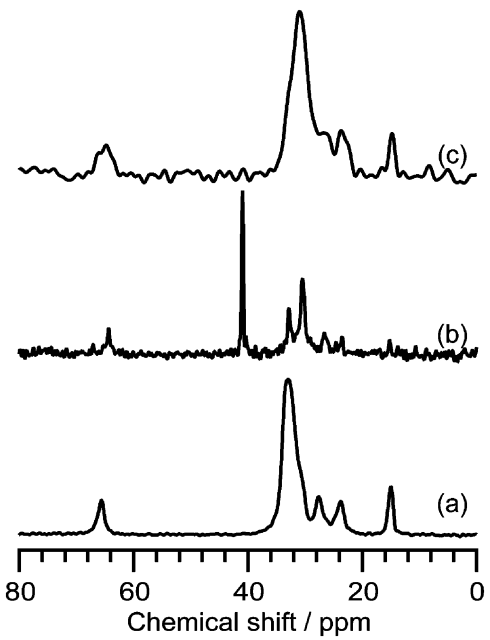

Fig. 5 ^{13}C CP/MAS NMR spectra of (a) **1(Ken)**, (b) **2(Ken)**, and (c) **3(Ken)**.

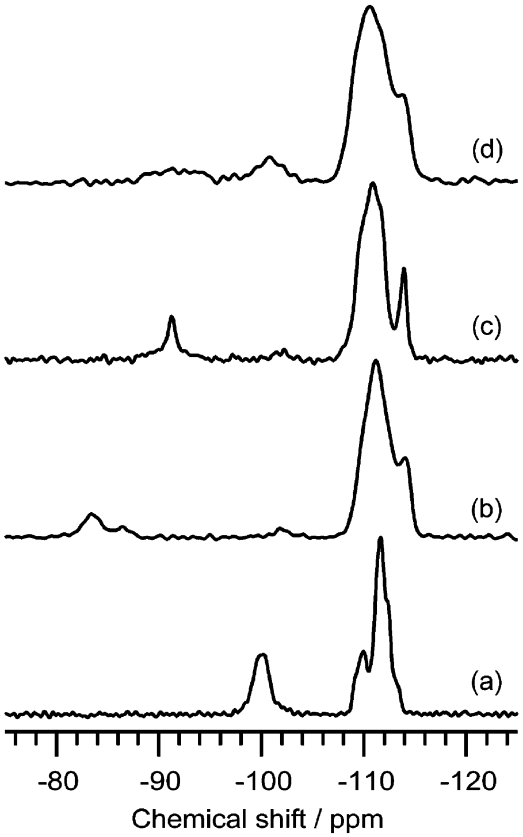

Fig. 6 ^{29}Si MAS NMR spectra of (a) C_{16}TMA-Mag, (b) **1(Mag)**, (c) **2(Mag)**, and (d) **3(Mag)**.

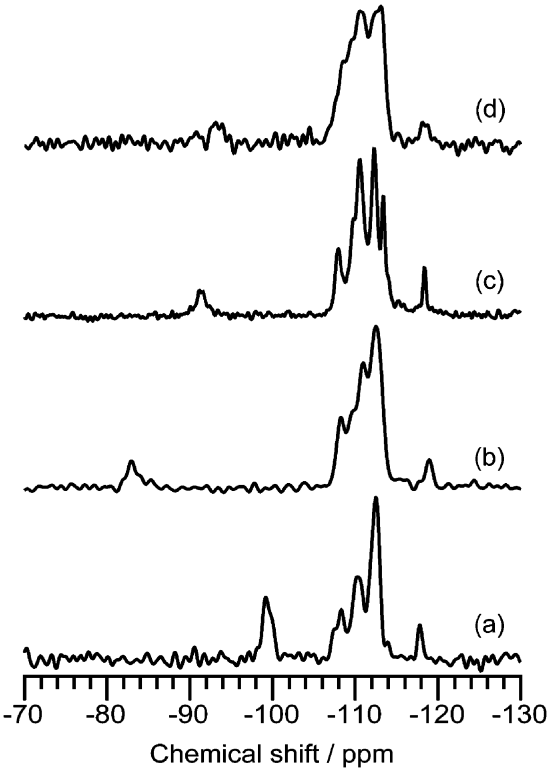

Fig. 7 ^{29}Si MAS NMR spectra of (a) C_{16}TMA-Ken, (b) **1(Ken)**, (c) **2(Ken)**, and (d) **3(Ken)**.

(Fig. 6b and 7b), and these signals can be ascribed to grafted alkoxysilyl groups [$Si(OSi)_2Cl(OR)$], designated as the I unit.[39] The shoulder signal at −86 ppm for the **1(Mag)** suggests the presence of the I unit with a different bonding state,[39] but it is difficult to determine it precisely due to the unknown silicate structure. The relative intensities of the I unit for **1(Mag)** and **1(Ken)** are 0.43 and 0.46 per one Si–OH (or $-O^-$) group (Q^3), respectively, which are in good agreement with the number of attached alkoxysilyl groups (*ca.* 0.50) per Si–OH (or $-O^-$) evaluated by TG and elemental analysis. The relative intensities of the Q^3 signal of the silylated samples decreased below 0.1, indicating that more than 90% of the reactive sites are silylated. In addition, the increases of the Q^4 signal per I signal [($Q^4 - 1$)/I] are 2.1 for **1(Mag)** and 2.2 for **1(Ken)**, which are attributed to the reaction of one alkoxytrichlorosilane molecule with two silanols of the layered silicates. The bridging reaction of alkoxytrichlorosilanes onto the silicate layers should be strongly affected by the lateral location of reactive sites. The distance of the neighboring reactive sites (Si–OH or Si–O^- groups) for magadiite has been determined to be 0.25 nm by the ^{1}H MAS NMR,[46] which is similar to that for octosilicate. Thus, it is supposed that magadiite has a suitable silicate structure for the bridging reaction by two Si–Cl groups of one alkoxytrichlorosilane. Additionally, the distance of neighboring silanol groups of kenyaite is presumably similar to that of octosilicate because of the same behavior of the alkoxysilylation.

Hydrolysis

The hydrolyzed products were obtained through the reaction of the silylated silicates with mixtures of a solvent and water. Here, the solvents are crucial to control the 2-D and 3-D nanostructures. To create 2-D silica nanostructures, DMSO was adopted as a solvent, because intercalated DMSO between hydrolyzed layers can suppress the condensation of adjacent layers due to its low volatility. The XRD patterns of **2(Mag)** and **2(Ken)** are shown in Fig. 2d and 3d, respectively. The d_{010} values decrease to 2.14 and 2.74 nm for **2(Mag)** and **2(Ken)**, respectively. Also, these patterns display different profiles in the higher angle region (2θ = 10–60°), revealing a high

Table 2 Relative intensity in the ^{29}Si MAS NMR spectra for the products

	I	Q^2	Q^3	Q^4	Q^4 generated by silylation[a]/I
C_{16}TMA-Mag	—	—	1.00	3.00	
1(Mag)	0.43	—	0.08	3.92	2.1
2(Mag)	—	0.47	0.09	3.88	
3(Mag)	—	—	0.53	3.88	
C_{16}TMA-Ken	—	—	1.00	5.25	
1(Ken)	0.45	—	—	6.25	2.2
2(Ken)	—	0.45	—	6.26	
3(Ken)	—	0.42	—	6.29	

[a] The increase in the intensity of Q^4 units generated by silylation was evaluated by subtraction of the intensity of the original Q^4 units of the C_{16}TMA intermediates from the intensities of the silylated products.

ordering of the silicate frameworks. The SEM images of layered silicates, the intermediates, the silylated samples, and the hydrolyzed samples (see ESI Fig. S1†) reveal that the morphologies of layered silicates are preserved during the silylation and hydrolysis processes. The carbon contents in **2(Mag)** and **2(Ken)** are 6.8 and 8.6 wt%, respectively, being smaller than those of the silylated products (Table 1). The ^{13}C CP/MAS NMR spectra (Fig. 4b and 5b) reveal the appearance of the signal due to DMSO (40 ppm) with the substantial decrease in the signal due to the alkoxy groups (*), indicating the hydrolysis of the interlayer alkoxy groups. Typically, the spectrum of **2(Mag)** shows a shoulder signal of DMSO at 43 ppm that is presumably ascribed to keyed methyl groups in the siloxane rings,[52] suggesting that the silicate layer of **2(Mag)** has an uneven surface. The uneven surface of magadiite has been supposed by the IR and ^{1}H NMR spectra of magadiite.[47,53] Fig. 6c and 7c show the ^{29}Si MAS NMR spectra of the hydrolyzed products. The signal corresponding to the SiCl(OR) groups (−84 ppm) was not observed in either of the spectra. The spectra of **2(Mag)** and **2(Ken)** show a new signal at −91 ppm, attributed to the Q^2 units possessing geminal silanol groups [$(SiO)_2Si(OH)_2$],[39] and the intensity is approximately equal to that of the I unit in the silylated derivatives. These quantitative transformations from I to Q^2 units indicate the creation of new 2-D silicate nanostructures without interlayer condensation.

On the other hand, the formation of a 3-D silica nanostructure is expected on using acetone as a solvent. The XRD patterns of **3(Mag)** and **3(Ken)** show the d_{010} values of 1.56 and 2.16 nm, respectively (Fig. 2e and 3e). The interlayer galleries of the samples were evaluated to be 0.40 and 0.51 nm, suggesting that the attached silyl groups were retained onto the layer surface. The carbon contents of the samples decreased from those of the silylated samples. The ^{13}C CP/MAS NMR spectra of the samples also show the substantial decrease of the alkoxy groups. These data indicate that the alkoxy groups were almost hydrolyzed and removed during the reaction. Additionally, the spectrum of **3(Mag)** shows the signals at 30 and 217 ppm corresponding to acetone molecules, although the spectrum of **3(Ken)** shows no signals in these regions. The ^{29}Si MAS NMR spectrum of **3(Mag)** showed the reappearance of Q^3 units at −101 ppm and unchanged retention of Q^4 units at −110 ppm. The newly formed Q^3 site in **3(Mag)** probably resulted from the hydrolysis of the alkoxy groups in **2(Mag)** and the subsequent condensation of the Si–OH groups between adjacent layers, because the Q^3 site in **3(Mag)** approximately equivalent to I unit in **1(Mag)** was observed. On the other hand, the ^{29}Si NMR spectrum of **3(Ken)** showed the signals at −92 and −110 ppm corresponding to the Q^2 and Q^4 units. The signal of Q^2 units is broader than that of **2(Ken)**, which may be due to the restriction of the attached Si species by the narrow interlayer gallery. The presence of the Q^2 unit with the intensity approximately equivalent to the I unit in **2(Ken)** reveals that the condensation of Si–OH groups between adjacent layers did not occur after the hydrolysis, resulting in the formation of a 2-D structure, although the ^{13}C CP MAS spectrum of **3(Ken)** shows the absence of acetone molecules within the interlayer spaces. The reason why interlayer condensation did not occur in this case

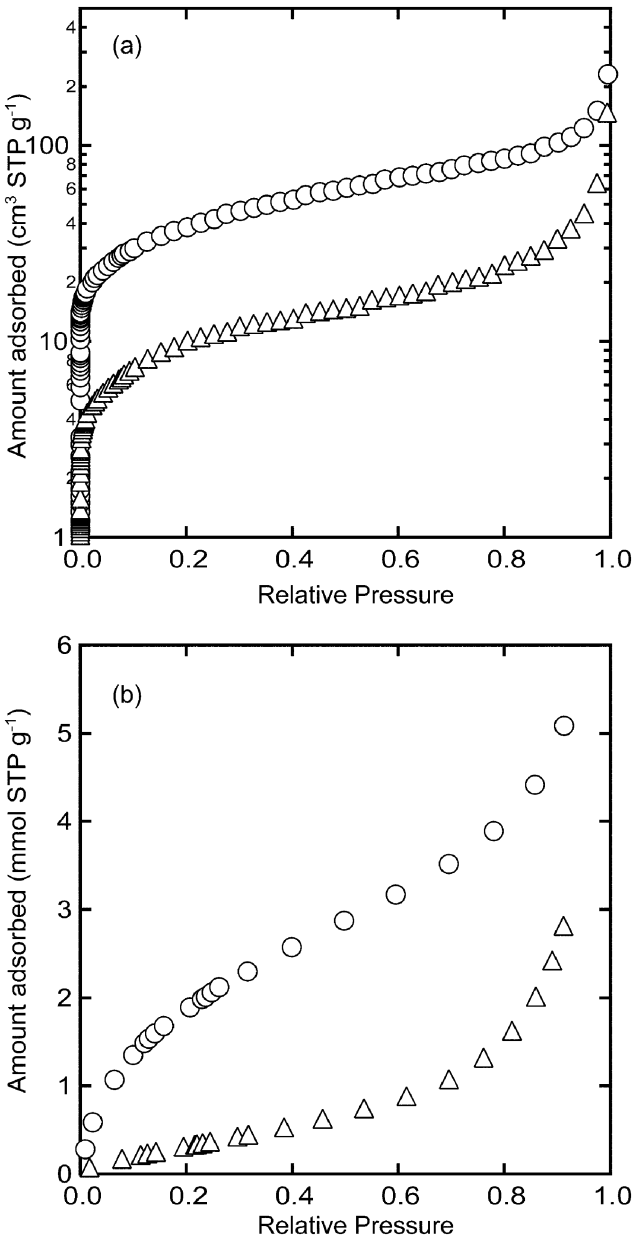

Fig. 8 Gas adsorption isotherms of (a) argon, and (b) H_2O. Circles and triangles correspond to **3(Mag)** and protonated magadiite, respectively.

can be explained as follows. The difference in the generated silicate nanostructures might be caused by the difference in the arrangement and/or alignment of Si–OH groups on kenyaite. Here, we can assume that the densities of Si–OH groups are similar among octosilicate, magadiite, and kenyaite, because the interlayer spaces of the silylated samples exhibited the same behavior (the degree of the increase in the interlayer gallery and conformation of alkoxy groups). Therefore, we consider that the arrangement and/or alignment of Si–OH groups on the layer surface of kenyaite are more complicated than those of other layered silicates. In fact, acid-treated H-kenyaite having interlayer silanol groups without condensation is known as a stable phase.[54] The delamination of layers

might also occur during the reaction in the case of **3(Ken)**, possibly resulting in the absence of condensation. However it is quite difficult to clarify these points.

To evaporate acetone molecules in **3(Mag)**, the sample was dried under vacuum at 200 °C. The XRD pattern of this sample shows a strong peak at the *d* value of 1.54 nm with several peaks. The removal of acetone was confirmed by the ^{13}C CP/MAS NMR spectrum of the sample. These data indicate that the ordered siloxane frameworks are retained after the removal of acetone. When octosilicate was used, the silicate frameworks collapsed after the removal of occluded acetone. Different from the case of octosilicate, the retention of the ordered siloxane frameworks implies the presence of a large aperture in the 3-D siloxane frameworks. Fig. 8a shows the argon adsorption isotherms of H-magadiite and **3(Mag)**. The shape of the isotherm for **3(Mag)** corresponds to type I in IUPAC classification, being characteristic of a microporous material. The Brunauer–Emmett–Teller (BET) surface area and the pore volume of **3(Mag)** were calculated to be 130 m^2 g^{-1} and 0.04 cm^3 g^{-1}, respectively. These values are lower than those of FER zeolites derived from topotactic conversion ($\sim$300 m^2 g^{-1} and 0.13 cm^3 g^{-1}),[11] possibly owing to the thicker silica walls and the residual alkoxy groups. The pore diameter calculated by the density functional theory was 5.2 Å which is slightly larger than the interlayer gallery ($\sim$4 Å). Here, we suppose that the accessible porosity was formed by the condensation of the adjacent layers composed from an uneven interlayer surface structure as suggested by the ^{13}C CP/MAS NMR spectra of **2(Mag)**. The uneven interlayer surface structure is likely to enlarge the aperture of the 3-D silicate structure, consequently leading to the formation of microporous materials. Actually, some of layered silicates such as makatite[55] and α-$Na_2Si_2O_5$[56] are composed of uneven silicate structures. Moreover, the hydrophilicity of **3(Mag)** was confirmed by the larger amount of water vapor as shown in Fig. 8b. Generally, the hydrophilicity of zeolites was attributed to the amounts of OH groups on the pore surface. We consider that this method provides OH-rich surfaces because of the soft-chemical conditions. Interestingly, the above results demonstrate the siloxane networks of hydrolyzed products from octosilicate, magadiite, and kenyaite are different each other, suggesting the intrinsic structural differences in the original layered silicates.

Conclusions

We have succeeded in synthesizing well designed silica nanostructures by interlayer alkoxysilylation of magadiite and kenyaite and the subsequent hydrolysis of the grafted groups. The layered silicates are silylated by alkoxytrichlorosilane in a well-regulated manner, resulting in the ordered grafting of alkoxychlorosilyl groups onto the interlayer surfaces. After the hydrolysis with a mixture of DMSO and water, the nanostructures derived from both magadiite and kenyaite are transformed into new layered silicates having interlayer geminal Si–OH groups. The different nanostructures are formed by the treatment with a mixture of acetone and water. The nanostructure derived from magadiite has a 3-D microporosity by the condensation of adjacent layers. On the other hand, the nanostructure from kenyaite retains the 2-D structure without condensation. This difference is possibly attributed to the original layered silica structures. The interlayer surface structure of layered silicates is a crucial issue for the precise control of structures as well as properties. We have shown two examples of the formation of silicate nanostructures by the controlled silylation and the following hydrolysis. Various crystalline nanobuilding units other than layered silicates should also be utilizable for this technique, which will be useful for designing novel nanostructures composed of nanocrystalline units.

Acknowledgements

This work is supported in part by a Grant-in-Aid for Center of Excellence (COE) Research "Molecular Nano-Engineering," the 21st Century COE Program "Practical Nano-Chemistry", and Encouraging Development Strategic Research Centers Program "Establishment of Consolidated Research Institute for Advanced Science and Medical Care" from the Ministry of Education, Culture, Sports, Science and Technology (MEXT), Japanese government. D. M. is grateful to financial supports by a Grant-in-Aid for JSPS Fellows from MEXT.

References

1 M. E. Davis, *Nature*, 1996, **382**, 583.
2 M. E. Davis, *Nature*, 2002, **417**, 813.
3 R. M. Barrer, *Hydrothermal Chemistry of Zeolites*, Academic Press, London, 1982.
4 G. Lagaly, *Adv. Colloid Interface Sci.*, 1979, **11**, 105.
5 C. S. Cundy and P. A. Cox, *Chem. Rev.*, 2003, **103**, 663.
6 C. S. Cundy and P. A. Cox, *Microporous Mesoporous Mater.*, 2005, **82**, 1.
7 S. Shimizu, Y. Kiyozumi, K. Maeda, F. Mizukami, G. PalBorbely, R. M. Mihalyi and H. Beyer, *Adv. Mater.*, 1996, **8**, 759.
8 F. Kooli, Y. Kioyozumi and F. Mizukami, *New J. Chem.*, 2001, **25**, 1613.
9 Y. Ko, S. J. Kim, M. H. Kim, J. H. Park, J. B. Parise and Y. S. Uh, *Microporous Mesoporous Mater.*, 1999, **30**, 213.
10 E. M. Barea, V. Fornés, A. Corma, P. Bourges, E. Guillon and V. F. Puntes, *Chem. Commun.*, 2004, 1974.
11 T. Ikeda, Y. Akiyama, Y. Oumi, A. Kawai and F. Mizukami, *Angew. Chem., Int. Ed.*, 2004, **43**, 4892.
12 R. Millini, L. C. Carluccio, A. Carati, G. Bellussi, C. Perego, G. Cruciani and S. Zanardi, *Microporous Mesoporous Mater.*, 2004, **74**, 59.
13 D. L. Dorset and G. J. Kennedy, *J. Phys. Chem. B*, 2004, **108**, 15216.
14 L. D. Rollmann, J. L. Schlenker, S. L. Lawton, C. L. Kennedy and G. J. Kennedy, *Microporous Mesoporous Mater.*, 2002, **53**, 179.
15 L. Schreyeck, P. Caullet, J. C. Mougenel, J. L. Guth and B. Marler, *Microporous Mater.*, 1996, **6**, 259.
16 S. Zanardi, A. Alberti, G. Cruciani, A. Corma, V. Fornés and M. Brunelli, *Angew. Chem., Int. Ed.*, 2004, **43**, 4933.
17 Y. X. Wang, H. Gies, B. Marler and U. Müller, *Chem. Mater.*, 2005, **17**, 43.
18 B. Marler, N. Stroter and H. Gies, *Microporous Mesoporous Mater.*, 2005, **83**, 201.
19 K. Kosuge and A. Tsunashima, *J. Chem. Soc., Chem. Commun.*, 1995, 2427.
20 K. Kosuge and P. S. Singh, *Chem. Mater.*, 2000, **12**, 421.
21 P. T. Tanev and T. J. Pinnavaia, *Science*, 1996, **271**, 1267.
22 P. H. Thiesen, K. Beneke and G. Lagaly, *J. Mater. Chem.*, 2002, **12**, 3010.
23 E. Ruiz-Hitzky and J. M. Rojo, *Nature*, 1980, **287**, 28.
24 E. Ruiz-Hitzky, J. M. Rojo and G. Lagaly, *Colloid Polym. Sci.*, 1985, **263**, 1025.

25 T. Yanagisawa, K. Kuroda and C. Kato, *React. Solids*, 1988, **5**, 167.
26 T. Yanagisawa, K. Kuroda and C. Kato, *Bull. Chem. Soc. Jpn.*, 1988, **61**, 3743.
27 K. Endo, Y. Sugahara and K. Kuroda, *Bull. Chem. Soc. Jpn.*, 1994, **67**, 3352.
28 M. Ogawa, S. Okutomo and K. Kuroda, *J. Am. Chem. Soc.*, 1998, **120**, 7361.
29 M. Ogawa, M. Miyoshi and K. Kuroda, *Chem. Mater.*, 1998, **10**, 3787.
30 S. Okutomo, K. Kuroda and M. Ogawa, *Appl. Clay Sci.*, 1999, **15**, 253.
31 K. Isoda, K. Kuroda and M. Ogawa, *Chem. Mater.*, 2000, **12**, 1702.
32 T. C. Chao, D. E. Katsoulis and M. E. Kenney, *Chem. Mater.*, 2001, **13**, 4269.
33 A. Shimojima, D. Mochizuki and K. Kuroda, *Chem. Mater.*, 2001, **13**, 3603.
34 D. Mochizuki, A. Shimojima and K. Kuroda, *J. Am. Chem. Soc.*, 2002, **124**, 12082.
35 Z. Zhang, S. Saengkerdsub and S. Dai, *Chem. Mater.*, 2003, **15**, 2921.
36 I. Fujita, K. Kuroda and M. Ogawa, *Chem. Mater.*, 2003, **15**, 3134.
37 Y. Guo, Y. Wang, Q.-X. Yang, G.-D. Li, C.-S. Wang, Z.-C. Cui and J.-S. Chen, *Solid State Sci.*, 2004, **6**, 1001.
38 I. Fujita, K. Kuroda and M. Ogawa, *Chem. Mater.*, 2005, **17**, 3718.
39 D. Mochizuki, A. Shimojima, T. Imagawa and K. Kuroda, *J. Am. Chem. Soc.*, 2005, **127**, 7183.
40 H. P. Eugster, *Science*, 1967, **157**, 1177.
41 K. Beneke and G. Lagaly, *Am. Mineral.*, 1977, **62**, 763.
42 *Handbook of Layered Materials*, eds. M. Auerbach, K. Carrado and P. K. Dutta, Marcel Dekker, New York, 2004, p. 541.
43 G. W. Brindley, *Am. Mineral.*, 1969, **54**, 1583.
44 T. J. Pinnavaia, I. D. Johnson and M. Lipsicas, *J. Solid State Chem.*, 1986, **63**, 118.
45 A. Brandt, W. Schwieger and K.-H. Bergk, *Cryst. Res. Technol.*, 1988, **23**, 1201.
46 C. Gardiennet and P. Takely, *J. Phys. Chem. B*, 2002, **106**, 8928.
47 J. M. Rojo, E. Ruiz-Hitzky and J. Sanz, *Inorg. Chem.*, 1988, **27**, 2785.
48 K. Kosuge, A. Yamazaki, A. Tsunashima and R. Otsuka, *J. Ceram. Soc. Jpn.*, 1992, **100**, 326.
49 O. Y. Kwon, S. Y. Jeong, J. K. Suh and J. M. Lee, *Bull. Korean Chem. Soc.*, 1995, **16**, 737.
50 E. Liepins, I. Zicmane and E. Lukevics, *J. Organomet. Chem.*, 1986, **306**, 167.
51 G. C. Ossenkamp, T. Kemmitt and J. H. Johnston, *Chem. Mater.*, 2001, **13**, 3975.
52 S. Hayashi, *J. Phys. Chem.*, 1995, **99**, 7120.
53 J. M. Rojo, E. Ruiz-Hitzky, J. Sanz and J. M. Serratosa, *Rev. Chim. Miner.*, 1983, **20**, 807.
54 K. Beneke and G. Lagaly, *Am. Mineral.*, 1983, **68**, 818.
55 H. Annehed, L. Faelth and F. J. Lincoln, *Z. Kristallogr.*, 1982, **159**, 203.
56 V. Kahlenberg, G. Dorsam, M. Wendschuh-Josties and R. X. Fischer, *J. Solid State Chem.*, 1999, **146**, 380.

